

Virus-mediated killing of cells that lack p53 activity

Kenneth Raj, Phyllis Ogston & Peter Beard

Swiss Institute for Experimental Cancer Research (ISREC),
155, Ch. des Boveresses, 1066 Epalinges, Switzerland

A major goal of molecular oncology is to identify means to kill cells lacking p53 function. Most current cancer therapy is based on damaging cellular DNA by irradiation or chemicals. Recent reports^{1,2} support the notion that, in the event of DNA damage, the p53 tumour-suppressor protein is able to prevent cell death by sustaining an arrest of the cell cycle at the G2 phase. We report here that adeno-associated virus (AAV) selectively induces apoptosis in cells that lack active p53. Cells with intact p53 activity are not killed but undergo arrest in the G2 phase of the cell cycle. This arrest is characterized by an increase in p53 activity and p21 levels and by the targeted destruction of CDC25C. Neither cell killing nor arrest depends upon AAV-encoded proteins. Rather, AAV DNA, which is single-stranded with hairpin structures at both ends^{3,4}, elicits in cells a DNA damage response that, in the absence of active p53, leads to cell death. AAV inhibits tumour growth in mice. Thus viruses can be used to deliver DNA of unusual structure into cells to trigger a DNA damage response without damaging cellular DNA and to selectively eliminate those cells lacking p53 activity.

Saos-2 cells (a p53-null, pRb-null osteosarcoma line) and U2OS cells (which are wild type for p53 and pRb) were infected with AAV-2. Saos-2 cells died, while U2OS cells did not die but enlarged (see Supplementary Information). To exclude replication of the AAV, ultraviolet-inactivated viruses were tested and found to give similar results. Ultraviolet-inactivated AAV was used for all subsequent experiments. Flow cytometry revealed that Saos-2 cells, when infected with AAV, accumulated briefly with 4n DNA content. Cell death occurred soon after (Fig. 1a). Many of these cells contained a quantity of DNA less than 2n (Fig. 1a), which together with Annexin V staining (data not shown) showed that they underwent apoptosis. However, most infected U2OS cells arrested with 4n DNA content and re-entered the cell cycle after several days (Fig. 1b). A minority of cells arrested with 2n DNA content. When higher amounts of AAV were used, most of the U2OS cells arrested

for a prolonged period (Fig. 1c). Whereas lower amounts of virus were sufficient to kill Saos-2 or transiently arrest U2OS cells (Fig. 1a and b), higher amounts were used to prolong the arrest and facilitate analysis of the arrested cells. To investigate the contribution of p53 activity in the response of cells to AAV infection, we inactivated the p53 protein in U2OS by ectopically overexpressing p53DD, a trans-dominant negative p53 mutant⁵. Infection of these cells with AAV resulted in a transient G2 arrest followed by cell death, as seen with Saos-2 cells (Fig. 1d).

When normal human osteoblasts (NHOs) were infected with AAV, they also enlarged and arrested with 4n DNA content (Fig. 1e). When the p53 protein in NHOs was degraded by expression of the human papilloma virus 16 (HPV-16) E6 protein before infection with AAV, the cells arrested at G2 for a short period before dying (Fig. 1f). These observations show that the effect of AAV is not unique to osteosarcomas but is also observable in normal osteoblasts, and that the outcome of this infection is dependent on p53 activity. Consistent with this, the p53 protein in U2OS was stabilized after AAV infection (Fig. 2a). A similar increase was also observed for the p21 protein (Fig. 2a), which is indicative of an increase in p53 activity⁶.

To analyse further the cell cycle block imposed by AAV, we assayed the activity of the cyclin B-cdc2 kinase complex, which triggers the G2/M transition of the cell cycle⁷. Cells blocked in mitosis by nocodazole exhibited high cyclin B-cdc2 kinase activity (Fig. 2b). However, AAV-infected U2OS and Saos-2 cells, despite having a 4n DNA content, possessed cyclin B-cdc2 kinase activity that was even lower than that of the unsynchronized control population, indicating that the AAV-induced block was at the G2 phase. Following infection of U2OS with AAV, a substantial fraction of the cdc2 protein migrated on gel electrophoresis at a slower rate than the control, indicating that it might be phosphorylated (Fig. 2c). Cells treated with nocodazole did not show the reduced migration of cdc2 protein, further suggesting that AAV does not induce an arrest in mitosis. Upon checking the protein level of CDC25C, a phosphatase crucial for activating cdc2 (ref. 8), we found that it decreased dramatically in AAV-infected U2OS (Fig. 2d) but not in AAV-infected U2OS+p53DD cells (Fig. 2e). This disappearance of CDC25C protein was prevented by N-acetyl-leu-leu-norleucinal (NaLLN)⁹, indicating involvement of the proteasome complex (Fig. 2f). This degradation was specific as the level of CDC25B protein (Fig. 2d) and that of many other proteins tested were unchanged.

To determine whether AAV could elicit these effects on other cell

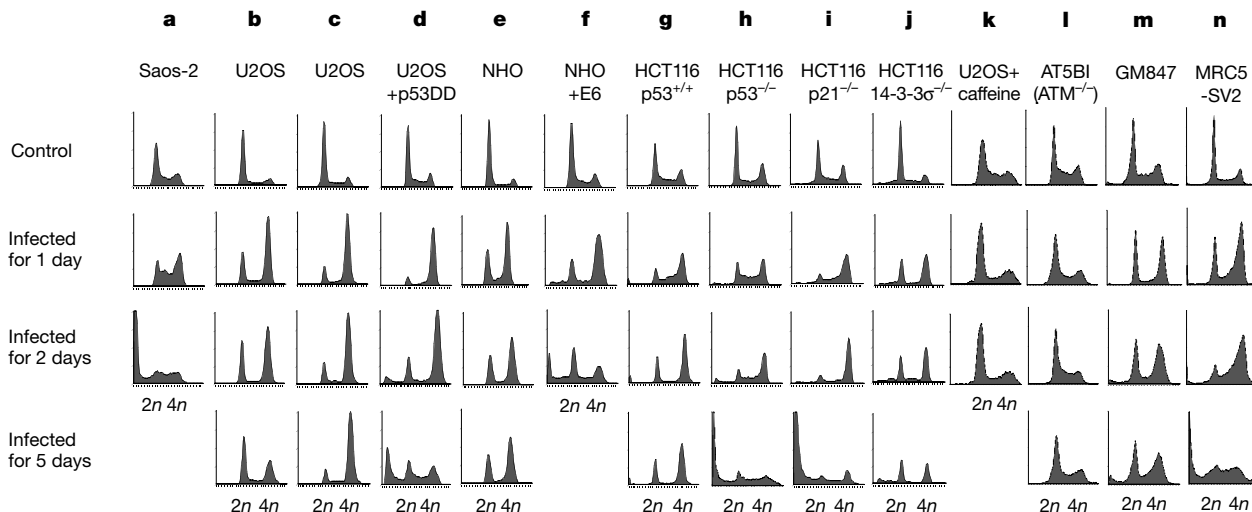


Figure 1 DNA content of cells after AAV infection. Cells were infected with AAV at a multiplicity of 250 (a and b) or 5,000 (c–n). After the indicated times, cells were collected and their DNA content measured by flow cytometry.

types, we infected a pair of isogenic human colon carcinoma cell lines, HCT116p53^{+/+} and HCT116p53^{-/-} (ref. 1), with AAV. Both the HCT116p53^{+/+} and HCT116p53^{-/-} cells arrested at the G2 phase of the cell cycle (Fig. 1g and h). However, the HCT116p53^{-/-} cells underwent cell death after several days (Fig. 1h). In AAV-infected HCT116p53^{+/+} cells, the levels of p53, p21 and 14-3-3σ proteins increased whereas that of CDC25C decreased (Fig. 2g). Interestingly, the level of CDC25C protein in HCT116p53^{-/-} cells, like that in the U2OS+p53DD cells, was unchanged after AAV infection (Fig. 2h), once again revealing the coupling of CDC25C protein

degradation to p53 activity. To test the relative importance of p21 and 14-3-3σ, HCT116 cells that lacked either of these proteins were infected with AAV. Cells lacking p21 failed to sustain the G2 arrest and died, while those lacking 14-3-3σ were still able to sustain the arrest with minimal cell death (Fig. 1i and j), underlining the importance of p21 in the G2 arrest.

The cellular responses to AAV and to DNA damage bear many similarities. In both cases, cells can respond either by establishing an arrest at G2 if p53 is present, or by pausing briefly at G2 before dying, when p53 is absent^{1,2}. We treated U2OS cells with etoposide, a DNA-damaging drug¹⁰, in place of AAV infection. When the levels of p53, p21 and CDC25C proteins were analysed, they were found to change in a manner similar to that caused by AAV (Fig. 2i). We know that, in response to DNA damage, nuclear localization of CDC25C is inhibited, inducing a G2 arrest¹¹. Our results reveal another mechanism for inactivation of CDC25C phosphatase: proteasomal degradation. An early step in DNA damage signalling can be mediated by the ATM protein¹². U2OS cells infected with AAV in the presence of the ATM inhibitor caffeine¹³ failed to arrest at the G2 phase, but continued to proliferate (Fig. 1k). Consistent with this, ATM-null cells (AT5BI, transformed with simian virus 40 (SV40)) were not affected by AAV. The SV40-transformed control cells (GM847 and MRC5-SV2) accumulated in G2 with cell death presumably depending on the level of residual p53 activity (Fig. 1l-n). These findings suggest that AAV affects the cell by inducing an ATM-dependent DNA damage response. Failure to induce this in ATM-null cells renders AAV ineffective in causing G2 arrest or apoptosis.

To test whether the incoming viral proteins were responsible for these effects, we used AAV-like particles without DNA we made using recombinant baculoviruses¹⁴, or empty AAV particles containing Rep, but not AAV DNA. When exposed to ultraviolet irradiation and added to cells, none of these affected cell growth (data not shown). Retroviral-mediated expression of the Rep proteins in cells did not induce the effects we saw with AAV¹⁵. The ultraviolet-inactivated AAV used here is unable to support the synthesis of viral proteins or DNA. As the effect of AAV on cells was not diminished by ultraviolet treatment, we conclude that viral replication or gene expression is not required for these effects. Ultraviolet-induced lesions in DNA were not responsible, as equivalent amounts of ultraviolet-inactivated adenovirus had no effect in parallel experiments (data not shown). Instead the evidence indicates that AAV DNA, which is single stranded with hairpin loops at both ends, can be sensed as abnormal DNA by the cell¹⁶ and trigger a DNA damage response. We tested this by injecting Saos-2, U2OS and U2OS+p53DD cells with an oligonucleotide corresponding to the AAV hairpin and containing no AAV coding sequence. This killed

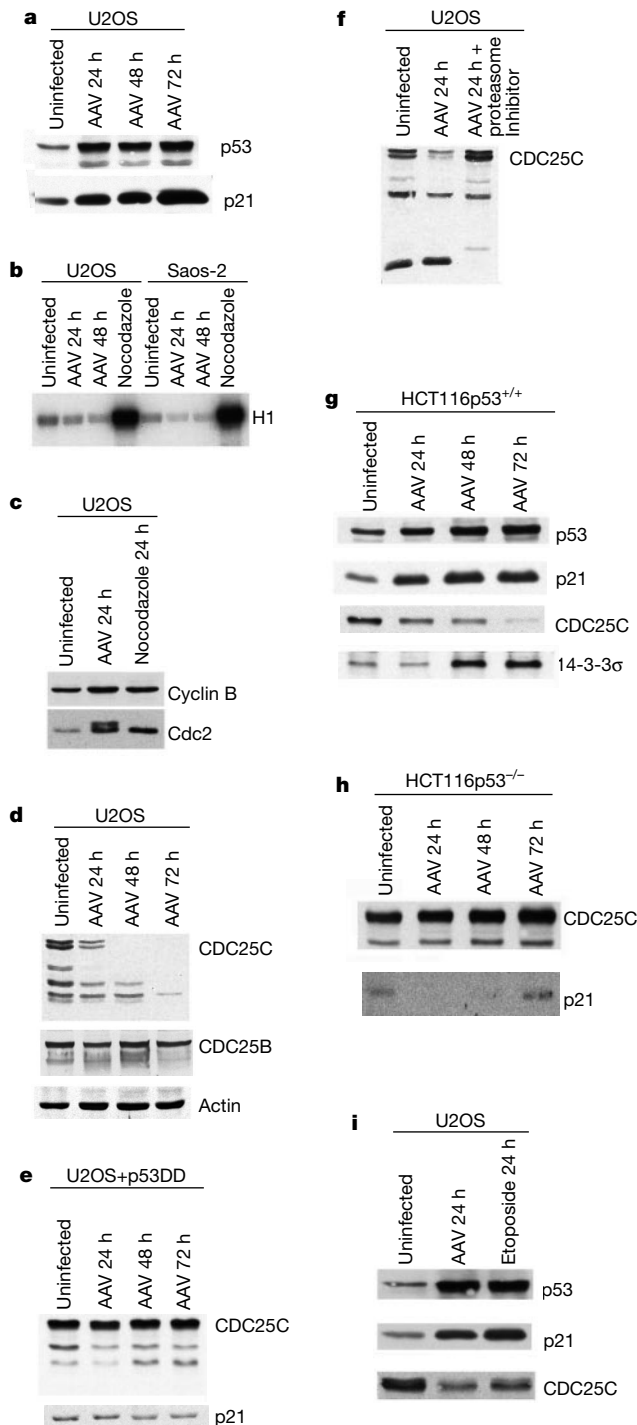


Figure 2 Biochemical analyses of proteins in AAV-infected cells. **a, c–i**, Western blotting analyses of various proteins in the indicated cell types. **b**, Cyclin B–cdc2 kinase assay of cells with and without AAV infection. H1, histone 1.

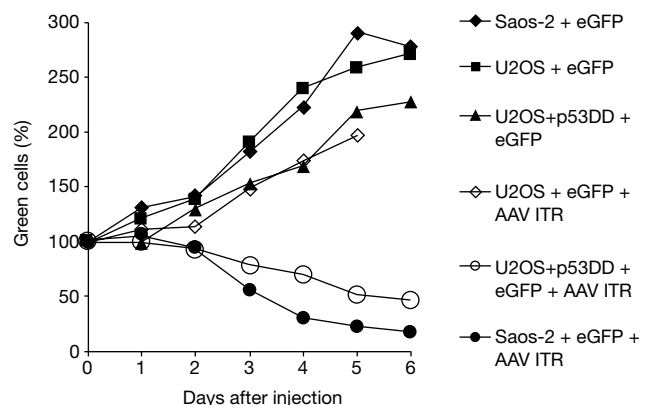


Figure 3 Cell viability following co-injection of AAV hairpin DNA (the inverted terminal repeat, ITR) and plasmids encoding green fluorescence protein (GFP) into different cell types.

Table 1 Effects of AAV on growth of tumours in athymic mice

Effect of AAV on tumour formation			
Cells	Treatment	Tumour incidence	Tumour incidence (%)
HCT116p53 ^{-/-}	PBS	12 of 12	100
	AAV	2 of 12	16.6
HCT116p53 ^{+/+}	PBS	10 of 10	100
	AAV	8 of 10	80
Effect of AAV on established tumours			
Tumours	Treatment	Number of tumours	Relative tumour volume (%)
HCT116 p53 ^{-/-}	PBS	10	100
	AAV	10	34–73
HT29	PBS	10	100
	AAV	4 6	19–34 0

the Saos-2 and U2OS+p53DD cells but not the U2OS cells (Fig. 3), supporting the conclusion that it is indeed the DNA of AAV that triggers a DNA damage response in the cells.

We tested whether this mechanism may be used to prevent the establishment of tumours. HCT116p53^{-/-} or HCT116p53^{+/+} cells were injected under the skin of nude mice, followed by injection of AAV, or PBS as a control, 2 days later. All of the control HCT116p53^{-/-} injections gave rise to tumours. Tumour incidence was reduced to 17% when AAV was used. HCT116p53^{+/+} cells were more resistant to AAV, as 80% of injections still produced tumours when AAV was present (Table 1 and see Supplementary Information). No non-specific toxicity was observed. This result is consistent with the observation¹⁷ that defective AAV particles that contained sub-genomic-length DNA with terminal hairpins protected hamsters against adenovirus-induced tumours. DNA fragments extracted from these defective particles were also able to prevent tumorigenesis. We then asked whether AAV is able to prevent the growth of pre-existing tumours lacking p53. Injection of AAV into established HCT116p53^{-/-} tumours inhibited their growth, resulting in tumours smaller than those injected with PBS. AAV injected into tumours derived from HT29, another p53-null colon carcinoma cell line, caused complete regression of 60% of the tumours and suppressed the growth of the remainder (Table 1 and see Supplementary Information).

How human tumours that lack p53 activity die in response to therapy remains puzzling¹⁸. Activation of p53 is often considered to lead to cell death, notably in lymphocytes¹⁹. However, there are cell types and situations where the presence of p53 prevents cell death by DNA damage^{1,2,19}. As irradiation and genotoxic drugs cause physical damage to cellular DNA, it was proposed that when damaged p53-null cells attempt to divide, they undergo mitotic catastrophe². In the experiments described above, we induced a DNA damage response using AAV instead of damaging the DNA of the cell, and observed that cells which lack p53 activity arrest transiently and die, suggesting that they possess a checkpoint that triggers apoptosis if they fail to sustain a G2 arrest in the face of DNA damage signalling. The absence of damaged cellular DNA may also explain why the ATM^{-/-} cells did not establish a delayed G2 arrest, as reported for certain ATM^{-/-} cells following irradiation²⁰.

Whereas further work will elucidate what kind of DNA damage AAV DNA is mimicking and details of which pathway is being triggered, the immediate importance of these findings is the introduction of the principle of using viruses to efficiently deliver DNA with unusual or modified structures into cells to eliminate those cells that lack p53 activity. □

Methods

Cell culture and inactivation of p53 *in vivo*

U2OS and Saos-2 cells were cultured in DMEM supplemented with 10% fetal calf serum. NHO cells were purchased from Clonetics and were cultured in Osteoblast Growth

Medium (Clonetics) supplemented with 10% fetal calf serum and ascorbic acid. DNA encoding the p53DD protein was cloned into the retroviral vector pBabepuro. To inhibit ATM activity, cells were treated with 2 mM caffeine. Annexin V analysis was performed according to the instructions of the manufacturer (Boehringer).

Inactivation of AAV and infection of cells

AAV prepared as described²¹ was diluted in 0.5 ml PBS in a small plastic dish and exposed to 2,400 J m⁻² of ultraviolet irradiation (wavelength 254 nm) from a Stratalinker. The inactivated viruses were further diluted in 2.5 ml DMEM (10% FCS) before adding them to cells. After 3 h, fresh medium was added to make up 10 ml.

Flow cytometry

Cells were gathered and fixed in 70% ethanol. Fixed cells were centrifuged, resuspended and incubated in 100 µg ml⁻¹ RNase in PBS at 37 °C. After 30 min, propidium iodide was added to a concentration of 100 µg ml⁻¹. DNA content was measured with a flow cytometer.

Western blotting and cyclin B-cdc2 kinase assay

Cells were washed twice with PBS and collected with a rubber-covered rod. After centrifugation cell pellets were resuspended in two volumes of Reporter Lysis Buffer (Promega) supplemented with a cocktail of protease inhibitors (Calbiochem). After incubation on ice for 30 min with occasional swirling, the samples were centrifuged at 16,100 g for 10 min. Supernatants were collected and protein concentrations measured by the Bradford assay (BioRad). Protein samples of 30 µg were resolved on SDS-polyacrylamide gels, transferred to nylon membranes (Hybond) and analysed with antibodies against p53, p21, CDC25C, CDC25B, actin, cyclin B and cdc2 (all from Santa Cruz). Cyclin B-cdc2 kinase assays were performed as described²².

Injection of cells

DNAs used in these experiments were first passed through a 0.2-µm filter. pCieGFP is a plasmid that contains a CMV promoter which controls the expression of the green fluorescent protein gene. The AAV hairpin oligonucleotide was synthesized (Microsynth) based on the sequence of the AAV-2 inverted terminal repeat (nucleotide positions 1–145). DNAs (either pCieGFP at 400 µg ml⁻¹, or pCieGFP at 200 µg ml⁻¹ with hairpin DNA at 200 µg ml⁻¹) were injected into cells with an Eppendorf Micromanipulator. Green cells were visible 4 h after injection and were then counted on successive days.

Received 30 March; accepted 11 June 2001.

- Bunz, F. *et al.* Requirement for p53 and p21 to sustain G2 arrest after DNA damage. *Science* **282**, 1497–1501 (1998).
- Chan, T. A., Hermeeking, H., Lengauer, C., Kinzler, K. W. & Vogelstein, B. 14-3-3σ is required to prevent mitotic catastrophe after DNA damage. *Nature* **401**, 616–620 (1999).
- Srivastava, A., Lusby, E. W. & Berns, K. I. Nucleotide sequence and organisation of the adeno-associated virus 2 genome. *J. Virol.* **45**, 555–564 (1983).
- Berns, K. I. & Linden, R. M. The cryptic life cycle of adeno-associated virus. *Bioessays* **17**, 237–245 (1995).
- Bowman, T. *et al.* Tissue specific inactivation of p53 tumour suppression in the mouse. *Genes Dev.* **10**, 826–835 (1996).
- Xiong, Y. *et al.* p21 is a universal inhibitor of cyclin-dependent kinases. *Nature* **366**, 701–704 (1993).
- Nurse, P. Universal control mechanism regulating cell cycle timing in M-phase. *Nature* **344**, 503–508 (1990).
- Strausfeld, U. *et al.* Activation of p34cdc2 protein kinase by microinjection of human CDC25C into mammalian cells. Requirement for prior phosphorylation of cdc25C by p34cdc2 on sites phosphorylated at mitosis. *J. Biol. Chem.* **269**, 5989–6000 (1994).
- Rock, K. *et al.* Inhibitors of the proteasome block the degradation of most cell proteins and the generation of peptides presented on MHC class I molecules. *Cell* **78**, 761–771 (1994).
- Wozniak, A. J. & Ross, W. E. DNA damage as a basis for 4'-demethylpiperidopylloxin-9-(4,6-O-ethylidene-beta-D-glucopyranoside) (etoposide) cytotoxicity. *Cancer Res.* **43**, 120–124 (1983).
- Peng, C. Y. *et al.* Mitotic and G2 checkpoint control regulation of 14-3-3 protein binding by phosphorylation of CDC25C on serine-216. *Science* **277**, 1501–1505 (1997).
- Rotman, G. & Shiloh, Y. ATM: a mediator of multiple responses to genotoxic stress. *Oncogene* **18**, 6135–6144 (1999).
- Blasina, A., Price, D. D., Turenne, G. A. & Gowen, C. H. Caffeine inhibits the checkpoint kinase ATM. *Curr. Biol.* **9**, 1135–1138 (1999).
- Ruffing, M., Zentgraf, H. & Kleinschmidt, J. A. Assembly of viruslike particles by recombinant structural proteins of adeno-associated virus type 2 in insect cells. *J. Virol.* **66**, 6922–6930 (1992).
- Saudan, P., Vlach, J. & Beard, P. Inhibition of S-phase progression by adeno-associated virus is mediated by hypophosphorylated pRb. *EMBO J.* **19**, 4351–4361 (2000).
- Yang, D., van Boom, S. S., Reedijk, J., Farrell, N. & Wang, A. H. A novel DNA structure induced by the anticancer bisplatinum compound crosslinked to a GpC site in DNA. *Nature Struct. Biol.* **2**, 577–578 (1995).
- De La Maza, L. M. & Carter, B. J. Inhibition of adenovirus oncogenicity in hamsters by adeno-associated virus DNA. *J. Natl Cancer Inst.* **67**, 1323–1326 (1981).
- Finkel, E. Does cancer therapy trigger cell suicide? *Science* **286**, 2256–2258 (1999).
- Brown, J. M. & Wouters, B. G. Apoptosis, p53, and tumour cell sensitivity to anticancer agents. *Cancer Res.* **59**, 1391–1399 (1999).
- Beamish, H. & Lavin, M. F. Radiosensitivity in ataxia-telangiectasia: anomalies in radiation-induced cell cycle delay. *Int. J. Radiat. Biol.* **65**, 175–184 (1994).
- Ogston, P., Raj, K. & Beard, P. Productive replication of adeno-associated virus can occur in human papillomavirus type 16 (HPV16) episome-containing keratinocytes and is augmented by the HPV16 E2 protein. *J. Virol.* **74**, 3494–3504 (2000).

22. Fournier, N. *et al.* Expression of human papillomavirus 16 E2 protein in *Schizosaccharomyces pombe* delays the initiation of mitosis. *Oncogene* **18**, 4015–4021 (1999).

Supplementary information is available on Nature's World-Wide Web site (<http://www.nature.com>) or as paper copy from the London editorial office of Nature.

Acknowledgements

We thank N. Paduwat and B. Bentele for technical assistance; M. Chapman and X. Qing for the gift of AAV-2; B. Vogelstein for the HCT116 cell line and its derivatives; R. Iggo for antibodies and the Saos-2 and U2OS cell lines; M. Oren for p53DD vectors; A. M. R. Taylor for the ATM-null cells; K. Alevizopoulos for retroviral vectors; J. Kleinschmidt for recombinant baculovirus; C. Wenz for assistance in insect cell culture; and S. Gasser, A.-L. Ducrest, M. Höss, B. Hirt, J. Jiricny, R. Iggo and V. Simanis for discussions. B. Sordat and F. Hoffmann helped with the animal experiments, and P. Reichenbach and J. Wyniger with the micro-injection. This work was supported by Cancer Research Switzerland and the Swiss National Science Foundation.

Correspondence and requests for materials should be addressed to P.B. (e-mail: peter.beard@isrec.unil.ch).

Rotational movement during cyclic nucleotide-gated channel opening

J. P. Johnson Jr & William N. Zagotta

Howard Hughes Medical Institute & Department of Physiology and Biophysics, Box 357290, University of Washington School of Medicine, Seattle, Washington 98195, USA

Cyclic nucleotide-gated (CNG) channels are crucial components of visual, olfactory and gustatory signalling pathways. They open in response to direct binding of intracellular cyclic nucleotides and thus contribute to cellular control of both the membrane potential and intracellular Ca²⁺ levels¹. Cytosolic Ni²⁺ potentiates the rod channel (CNG1) response to cyclic nucleotides^{2–4} and inhibits the olfactory channel (CNG2) response⁵. Modulation is due to coordination of Ni²⁺ by channel-specific histidines in the C-linker, between the S6 transmembrane segment and the cyclic nucleotide-binding domain. Here we report, using a histidine scan of the initial C-linker of the CNG1 channel, stripes of sites producing Ni²⁺ potentiation or Ni²⁺ inhibition, separated by 50° on an α-helix. These results suggest a model for channel gating where rotation of the post-S6 region around the channel's central axis realigns the Ni²⁺-coordinating residues of multiple subunits. This rotation probably initiates movement of the S6 and pore opening.

The mechanism of Ni²⁺ modulation is simple: Ni²⁺ binding is state dependent. Ni²⁺ is an intermediate Lewis acid and prefers association with intermediate Lewis bases, such as the imidazole of histidine⁶. In CNG1 channels, naturally bearing H420, the open channel has a higher affinity (>100 times) for Ni²⁺ than the closed channel, and Ni²⁺ promotes channel opening. In CNG2 channels, naturally bearing a histidine at the 417 equivalent position, the closed channel has higher affinity for Ni²⁺ than the open channel, and Ni²⁺ promotes channel closing (Fig. 1a)^{2,5}. Ni²⁺ affects the opening transition, but not the intrinsic ligand binding, as Ni²⁺ modulation is seen even in the presence of saturating concentrations of partial agonists where binding sites are maximally occupied^{2,3,7}. Individual histidines bind Ni²⁺ poorly (~1 mM), but multiple histidines, especially in a square planar geometry, can coordinate Ni²⁺ with sub-micromolar affinity⁸. Ni²⁺ coordination in CNG1 channels occurs between two adjacent channel subunits^{9,10}.

Predictions of the secondary structure¹¹ suggest that the S6 and the C-linker of CNG1 channels are α-helical in nature until position 420. The KcsA K⁺ channel has been crystallized¹², providing a

structural model for the pores of other P-loop-containing cation channels, including CNG channels. To create a working model, we threaded the aligned amino-acid sequence of the S6 and P-loop of the CNG1 channel through the KcsA structure and extended the α-helix of the CNG1 channel S6 to position 420 (Fig. 1b). Residue 417 (Fig. 1b, red) points in the direction of the central axis, which allows Ni²⁺ coordination, while residue 420 (Fig. 1b, green) points away from the central axis. Rotation of the helix on channel opening could change the orientation of the residues such that residue 420 would point towards, and 417 away, from the central axis, thereby explaining state-dependent histidine coordination of Ni²⁺.

This model predicts that other positions near 417 and 420 in the post-S6 region might also be able to coordinate Ni²⁺. We completed a histidine scan between positions 403 and 420 in a Ni²⁺-insensitive CNG1 channel, H420Q (Fig. 2c right)^{2,5}. Each residue between position 403 and 420 was individually replaced with histidine, and cGMP dose-response curves were measured in the absence and presence of Ni²⁺.

We found three Ni²⁺ phenotypes: Ni²⁺-inhibited, Ni²⁺-potentiated and Ni²⁺-insensitive. Ni²⁺ inhibited three channels, Q409H, D413H and Q417H (Fig. 2a). For Q409H and D413H channels, Ni²⁺ caused a decrease in current at sub-saturating cGMP concentrations, causing the cGMP dose-response relationship to shift right (Fig. 2a, right). Q417H currents were completely inhibited by 1 μM Ni²⁺, even at saturating concentrations of cGMP, which made the measurement of cGMP dose responses in Ni²⁺ impossible⁵. Ni²⁺ potentiated two channels, K416H and H420 (Fig. 2b). Addition of Ni²⁺ to these channels increased the current, causing the cGMP dose-response relationship to shift left (Fig. 2b, right). Ni²⁺ had no effect on 11 out of 18 channel constructs (Fig. 2c). Two mutants (I415H and M419H) failed to produce currents in either the absence or presence of Ni²⁺.

To quantify the effect of intracellular Ni²⁺, we fit the cGMP dose-response relationships for all mutants (except D413H) in the absence and presence of Ni²⁺ with a simple allosteric model containing two ligand-binding events and an allosteric opening transition (see Methods). Although the model is oversimplified, it provides a reasonable fit of the data and a straightforward analysis.

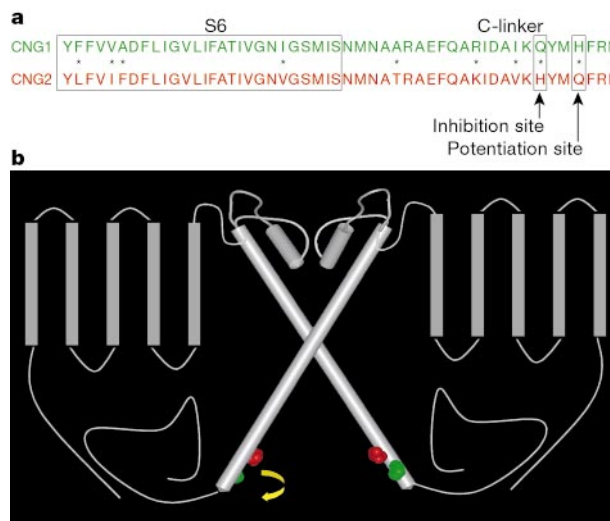


Figure 1 Ni²⁺-coordinating histidines. **a**, Sequence alignment showing the location of Ni²⁺-coordinating histidines in CNG1 and CNG2. Stars indicate nonconserved positions. **b**, Depiction of two of the four CNG1 channel subunits. S1–S5 transmembrane domains are represented by vertical grey rectangles. The cylinders representing the pore and S6 helices are the result of aligning the CNG1 sequence with the KcsA channel structure and extending the S6 to position 420, although sequence similarity with KcsA ends near the helical bundle crossing at 399. Residues 417 and 420 are coloured red and green, respectively.

non-taster alleles of T1R3 used constructs of complementary DNA coding for T1R3 from C57BL/6 and 129/Sv mice, respectively^{7–11,21}.

Immunoprecipitation

Antibodies against T1R3 were generated using a peptide corresponding to residues 824–845 of the mouse receptor. PEAK^{rapid} cells (Edge Biosciences) were transfected with HA–T1R1, HA–T1R2 and T1R3 in various combinations and were gathered and disrupted in buffer containing 50 mM Tris-HCl at pH 7.5, 300 mM NaCl, 1% NP-40, 0.5% w/v sodium deoxycholate, and protease inhibitors (Roche). Lysates were incubated overnight at 4 °C with mouse monoclonal anti-HA antibody (Santa Cruz) and immune complexes were collected with protein A/G–agarose beads. Samples were fractionated by SDS–PAGE, transferred to nitrocellulose membrane and probed with anti-T1R3 antibody. As a control for the specificity of the interactions, we have shown that artificially mixing extracts from cells expressing tagged T1R1 or T1R2 with extracts from cells expressing T1R3 does not produce complexes. Similarly, co-transfection of a Rho-tagged mGluR1 receptor¹⁵ did not produce T1R–GluR1 complexes.

Nerve recording

Lingual stimulation and recording procedures were performed as previously described²⁷. Neural signals were amplified (2,000 ×) with a Grass P511 AC amplifier (Astro-Med), digitized with a Digidata 1200B A/D converter (Axon Instruments), and integrated (r.m.s. voltage) with a time constant of 0.5 s. Taste stimuli were presented at a constant flow rate of 4 ml min⁻¹ for 20-s intervals interspersed by 2-min rinses between presentations. All data analyses used the integrated response over a 25-s period immediately after the application of the stimulus. Each experimental series consisted of the application of six tastants bracketed by presentations of 0.1 M citric acid to ensure the stability of the recording. The mean response to 0.1 M citric acid was used to normalize responses to each experimental series.

Received 21 January; accepted 7 February 2002.

Published online 24 February 2002, DOI 10.1038/n416031a.

- Lindemann, B. Taste reception. *Physiol. Rev.* **76**, 718–766 (1996).
- Iwasaki, K., Kasahara, T. & Sato, M. Gustatory effectiveness of amino acids in mice: behavioral and neurophysiological studies. *Physiol. Behav.* **34**, 531–542 (1985).
- Hoon, M. A. *et al.* Putative mammalian taste receptors: a class of taste-specific GPCRs with distinct topographic selectivity. *Cell* **96**, 541–551 (1999).
- Adler, E. *et al.* A novel family of mammalian taste receptors. *Cell* **100**, 693–702 (2000).
- Chandrasekar, J. *et al.* T2Rs function as bitter taste receptors. *Cell* **100**, 703–711 (2000).
- Matsunami, H., Montmayeur, J. P. & Buck, L. B. A family of candidate taste receptors in human and mouse. *Nature* **404**, 601–604 (2000).
- Nelson, G. *et al.* Mammalian sweet taste receptors. *Cell* **106**, 381–390 (2001).
- Kitagawa, M., Kusakabe, Y., Miura, H., Ninomiya, Y. & Hino, A. Molecular genetic identification of a candidate receptor gene for sweet taste. *Biochem. Biophys. Res. Commun.* **283**, 236–242 (2001).
- Montmayeur, J. P., Liberles, S. D., Matsunami, H. & Buck, L. B. A candidate taste receptor gene near a sweet taste locus. *Nature Neurosci.* **4**, 492–498 (2001).
- Max, M. *et al.* Tas1r3, encoding a new candidate taste receptor, is allelic to the sweet responsiveness locus Sac. *Nature Genet.* **28**, 58–63 (2001).
- Sainz, E., Korley, J. N., Battey, J. F. & Sullivan, S. L. Identification of a novel member of the T1R family of putative taste receptors. *J. Neurochem.* **77**, 896–903 (2001).
- Offermanns, S. & Simon, M. I. Gα₁₃ and Gα₁₆ couple a wide variety of receptors to phospholipase C. *J. Biol. Chem.* **270**, 15175–15180 (1995).
- Mody, S. M., Ho, M. K., Joshi, S. A. & Wong, Y. H. Incorporation of Gα₂-specific sequence at the carboxyl terminus increases the promiscuity of Gα₁₆ toward G_i-coupled receptors. *Mol. Pharmacol.* **57**, 13–23 (2000).
- Tsien, R. Y., Rink, T. J. & Poenie, M. Measurement of cytosolic free Ca²⁺ in individual small cells using fluorescence microscopy with dual excitation wavelengths. *Cell Calcium* **6**, 145–157 (1985).
- Nakanishi, S. Molecular diversity of glutamate receptors and implications for brain function. *Science* **258**, 597–603 (1992).
- Kaupmann, K. *et al.* Expression cloning of GABA_B receptors uncovers similarity to metabotropic glutamate receptors. *Nature* **386**, 239–246 (1997).
- Specia, D. J. *et al.* Functional identification of a goldfish odorant receptor. *Neuron* **23**, 487–498 (1999).
- Yoshii, K., Yokouchi, C. & Kurihara, K. Synergistic effects of 5′-nucleotides on rat taste responses to various amino acids. *Brain Res.* **367**, 45–51 (1986).
- Fuller, J. L. Single-locus control of saccharin preference in mice. *J. Hered.* **65**, 33–36 (1974).
- Lush, I. E. The genetics of tasting in mice. VI. Saccharin, acesulfame, dulcin and sucrose. *Genet. Res.* **53**, 95–99 (1989).
- Bachmanov, A. A. *et al.* Positional cloning of the mouse saccharin preference (Sac) locus. *Chem. Senses* **26**, 925–933 (2001).
- Bachmanov, A. A., Tordoff, M. G. & Beauchamp, G. K. Intake of umami-tasting solutions by mice: a genetic analysis. *J. Nutr.* **130**, 935S–941S (2000).
- Bachmanov, A. A., Tordoff, M. G. & Beauchamp, G. K. Sweetener preference of C57BL/6ByJ and 129P3/J mice. *Chem. Senses* **26**, 905–913 (2001).

- Ikeda, K. On a new seasoning. *J. Tokyo Chem. Soc.* **30**, 820–836 (1909).
- Kurihara, K. & Kashiwayanagi, M. Introductory remarks on umami taste. *Ann. NY Acad. Sci.* **855**, 393–397 (1998).
- Chaudhari, N., Landin, A. M. & Roper, S. D. A metabotropic glutamate receptor variant functions as a taste receptor. *Nature Neurosci.* **3**, 113–119 (2000).
- Dahl, M., Erickson, R. P. & Simon, S. A. Neural responses to bitter compounds in rats. *Brain Res.* **756**, 22–34 (1997).

Acknowledgements

We thank W. Guo for help generating various T1R expression constructs, and A. Becker for help with tissue culture and antibodies. We are grateful to S. Simon and R. Erikson for teaching us the nerve-recording preparation. We also thank L. Stryer and members of the Zuker lab for help and advice. This work was supported in part by a grant from the National Institute on Deafness and Other Communication Disorders to C.S.Z. C.S.Z. is an investigator of the Howard Hughes Medical Institute.

Competing interests statement

The authors declare that they have no competing financial interests.

Correspondence and requests for materials should be addressed to C.S.Z. (e-mail: charles@flyeye.ucsd.edu).

addendum

Virus-mediated killing of cells that lack p53 activity

Kenneth Raj, Phyllis Ogston & Peter Beard

Nature **412**, 914–917 (2001).

Some background information to our work on adeno-associated virus (AAV)-induced apoptosis in cells lacking p53 activity was omitted owing to space constraints. The oncosuppressive activity of parvoviruses has been reviewed^{1,2}. AAV inhibits cell cycle progression³, even when ultraviolet-inactivated⁴, as do AAV-coded Rep proteins⁵. p53-dependent cytopathic effects of parvovirus H1 have been reported⁶. H1 is an autonomous virus that can replicate in cells and lyse them. This is different from AAV, which is defective and does not replicate in the conditions we used. H1 and AAV share little sequence homology and the structures of the DNA termini are not the same. □

- Rommelaere, J. & Cornelis, J. J. Antineoplastic activity of parvoviruses. *J. Virol. Methods* **33**, 233–251 (1991).
- Schlehofer, J. The tumor suppressive properties of adeno-associated viruses. *Mutat. Res.* **305**, 303–313 (1994).
- Hermanns, J. *et al.* Infection of primary cells by adeno-associated virus type 2 results in a modulation of cell cycle-regulating proteins. *J. Virol.* **71**, 6020–6027 (1997).
- Winocour, E., Callahan, M. & Huberman, E. Perturbation of the cell cycle by adeno-associated virus. *Virology* **167**, 393–399 (1988).
- Saudan, P., Vlach, J. & Beard, P. Inhibition of S-phase progression by adeno-associated virus Rep78 protein is mediated by hypophosphorylated pRb. *EMBO J.* **19**, 4351–4361 (2000).
- Telerman, A. *et al.* A model for tumor suppression using H-1 parvovirus. *Proc. Natl Acad. Sci. USA* **90**, 8702–8706 (1993).